PERGAMON

International Journal of Solids and Structures 39 (2002) 741–763

INTERNATIONAL JOURNAL OF SOLIDS and STRUCTURES

www.elsevier.com/locate/ijsolstr

A thermodynamic constitutive model for stress induced phase transformation in shape memory alloys

Jiujiang Zhu [a], Naigang Liang [b], Weimin Huang [a,*], K.M. Liew [a], Zhihong Liu [b]

[a] *Centre for Advanced Numerical Engineering Simulations, Nanyang Technological University, Nanyang Avenue, Singapore 639798, Singapore*

[b] *LNM Institute of Mechanics, Chinese Academy of Sciences, Beijing 100080, China*

Received 12 November 1999; received in revised form 16 May 2001

Abstract

In this paper a thermodynamic constitutive model is developed for stress induced phase transformation in single crystalline and polycrystalline shape memory alloys (SMAs). Volume fractions of different martensite variants are chosen as internal variables to describe the evolution of microstructure state in the material. This model is then used in prediction the transformation behavior of a SMA (Cu–Al–Zn–Mn) under complex thermomechanical load (including complete and incomplete transformation in mechanical cycling, and proportional/non-proportional loading). © 2002 Elsevier Science Ltd. All rights reserved.

Keywords: Shape memory alloy; Martensitic transformation; Non-proportional loading; Constitutive model

1. Introduction

As a new type of functional material, shape memory alloy (SMA) has been exploited to be used in various applications (Funakubo, 1987). However, compared with other traditional materials, current research on the constitutive relation of SMAs is still far away from well established. In particular, the themomechanical behaviors described in the $(\boldsymbol{\sigma}, \boldsymbol{\varepsilon}, \boldsymbol{T})$ space under complex load is still under investigation. Related topics include the behavior under mechanical and thermal cyclic load, non-proportional load and the effects of loading history. In order to provide a robust tool for engineers, much attention has been attracted to SMA modeling in recent years. According to Boyd and Lagoudas (1996), previews models in the literature may be classified into two categories: two-component phenomenological model (e.g. Sun and Hwang, 1993), and three-component phenomenological model (e.g. Raniecke and Lexcellent, 1994; Leclercq and Lexcellent, 1996). In two-component phenomenological model, two phases, austenite and martensite, are considered. In three-component phenomenological model, martensite is further divided into self-accommodated (twinned) martensite and non-self-accommodated (detwinned) martensite. In order to establish the constitutive model, two assumptions are made in both types of models:

* Corresponding author.

0020-7683/02/$ - see front matter
PII: S0020-7683(01)00152-4

Nomenclature

A	coefficient of interaction energy
A_0	boundary of RVE
A_f	austenite finish temperature
A_s	austenite start temperature
A_{ij}	boundary of jth grain with orientation i
A_{ijkl}	boundary of V_{ijkl}
$\mathbf{b}_{il}$	shear vector of HPV
c_i	volume fraction of all crystals with orientation ith in RVE
C_V	specific heat
E_0	elastic modulus
$\mathbf{e}$	microscopic total strain
$\mathbf{e}^e$	microscopic elastic strain
$\mathbf{e}_{ijkl}$	microscopic total strain in volume V_{ijkl}
$\mathbf{e}^e_{ijkl}$	microscopic elastic strain in volume V_{ijkl}
$\mathbf{E}$	macroscopic total strain
$\mathbf{E}^e$	macroscopic elastic strain
$\mathbf{E}^{tr}$	macroscopic phase transformation strain
$\mathbf{E}^{tr}_{ik}$	phase transformation eigenstrain of kth type of LCV with orientation i
$\mathbf{E}^*_{il}$	Phase transformation eigenstrain of HPV
f^s	internal energy due to internal stress field $\boldsymbol{\sigma}_{int}$
f^s_i	internal energy in grains with orientation i
$\mathbf{F}$	surface force on A_0
g	magnitude of pure shear in HPV
G	specific Gibbs free energy
G_0	shear modulus
H	total number of HPVs in single crystal
h_0	entropy at temperature T_0
$\mathbf{L}$	elastic module tensor
$\mathbf{m}_{il}$	direction of pure shear in HPV
M_f	martensite finish temperature
M_i	total number of grains with orientation i
M_s	martensite start temperature
$\mathbf{M}$	elastic compliance tensor
n	number of martensite LCV
$\mathbf{n}$	normal direction of A_0
$\mathbf{n}_{il}$	normal direction of Habit plane
N	number of grain orientation
$\mathbf{P}_{il}$	orientation tensor of pure shear
Q_{ijk}	number of kth type of LCVs in volume V_{ij}
R	total number of orientation components
T_0	reference temperature
T^{eq}	phase equilibrium temperature
u	microscopic specific internal energy
u_0	free energy at temperature T_0
u_{ijkl}	specific internal energy in volume V_{ijkl}
U	macroscopic specific internal energy
V	volume of RVE
V_i	volume of all grains with orientation i
V_{ij}	volume of jth grain with orientation i
V_{ijkl}	volume of lth martensite crystal with kth type of LCVs in volume v_{ij}
W_{ik}	volume of all LCVs belong to kth group of orientation i
z_{ik}	volume fraction of kth group with orientation i
z^*_{il}	volume fraction of Habit Plane Variants

Greeks

ε	volume deformation of HPV
$\boldsymbol{\varepsilon}^{tr}$	microscopic eigenstrain of phase transformation
ϕ	microscopic elastic energy
Φ	macroscopic elastic energy
ϕ_{ijkl}	elastic energy in volume V_{ijkl}
η	microscopic specific entropy
η^*	specific local entropy production
λ	material constants to describe hardening behavior
μ	material constants to describe interaction among HPVs
v_{kl}	stoichiometric coefficient for forward phase transformation
Ξ_{ik}	driving force corresponding to z_{ik}
Π_{il}	driving force corresponding to z^*_{il}
Π^{c+}_{il}	critical driving force for forward transformation
Π^{c-}_{il}	critical driving force for reverse transformation
Π_0	minimum Π^{c+}_{il}
Θ_{il}	equivalent pressure in HPV

ρ	microscopic mass density	τ_{il}	resolved shear stress in HPV
ρ_t	macroscopic mass density of RVE	ζ	macroscopic specific entropy
$\boldsymbol{\sigma}_{ijkl}$	microscopic stress in volume V_{ijkl}		
$\boldsymbol{\sigma}_{\text{int}}$	internal stress caused by eigenstrain of phase transformation	*Superscript*	
		A	austenite
$\boldsymbol{\Sigma}$	macroscopic stress	M	martensite

(1) The direction of strain rate is the same as that of devoatoric stress. In the construction of free energy expression, this assumption is only true for proportional loading case.
(2) A thermodynamic dissipation potential function is postulated in construction the formula for evolution of phase transformation.

It is also noticed that in practice it is very hard to distinguish twinned martensite and detwinned martensite. In fact, it is the particular martensite variant, which has the most favorable orientation by local stress field, growing at the cost of other variants. Martensite variants with different orientation play an important role in both forward and reverse transformations. So it should be more accurate if different martensite variants are introduced as internal variables in modeling. Liang et al. (1995) has applied orientation component method in investigation the constitutive theory of SMAs. Later, this method was used in a submicroscopic elasto-plastic model for polycrystalline metals (Liang et al., 1998).

On the other hand, previews models, such as Boyd and Lagoudas (1996), Huang and Brinson (1998), appear to be complete and ideal theoretically. However most of the numerical simulations used for verification are simple loading case. Applying these models in non-proportional case, for instance, tests reported by Sittner et al. (1995), could be very complex.

In this paper, based on the thermodynamic theory of continuum, the macroscopic Gibbs free energy is derived from $n+1$ microscopic potential wells (n martensite variants plus one for austenite), and the thermodynamical force that corresponds to the volume fraction variation of martensite variant is derived. Nucleation criterion and evolution equation for phase transition process are proposed based on the observation in single martensite variant experiment reported by Huo and Müller (1993). An orientation component model is established for isotropic polycrystalline SMA. This model is then used in the simulation of a Cu–Al–Zn–Mn polycrystalline SMA round tube subjecting to complex loads and non-proportional loads tested by Sittner et al. (1995).

2. Model for phase transformation in SMA

Martensitic transformation is first order transformation from solid to solid. Macroscopically, such transformation results in phase transition, such as pseudoelasticity and shape memory effect, etc. Microscopically, phase transformation turns one austenite into mixture phase of autensite and martensite first, and pure martensite in the end. As the symmetry of autensite is of higher order than that of martensite, a group of martensite variants may be generated from one austenite. The resulting single martensite crystal is martensite lattice correspondence [1] variant (LCV). In terms of free energy, "n" number of LCVs forms "n"

[1] A lattice correspondence is a unique relationship between the initial (austenite) and final (martensite) lattices.

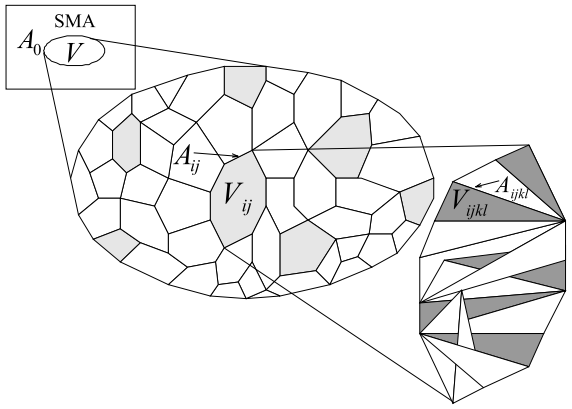

Fig. 1. Scale illustration. The gray areas in the middle figure stand for grains with same orientation in austenite. The black areas in right figure represent martensite with the same type of lattice corresponding variant.

potential wells. Plus one for austenite, "$n+1$" potential wells exist in SMA. Although microscopically deformation may not be continuous everywhere, displacement is continuous. Hadamard jump condition becomes internal geometrical restraint. To satisfy this, interface between martensite LCVs must be twinned plane, while interphase between austenite and martensite must be habit plane (refer to Ball and James, 1987; Bhattacharya, 1992). On the martensite side of habit plane it is martensite habit plane variant (HPV). It is well known that HPV is not always the minimum subunit that composes the bulk martensite. In some SMAs, for instance CuZnAl, HPV is LCV. But in some others, such as TiNi and CuAlNi, HPV composes two twin-related LCVs (refer to Saburi and Nenno, 1982 for details). Thus, LCV should be potential well instead of HPV. This issue is not recognized in most of the previous models.

Consider a piece of stress-free polycrystalline SMA as shown in Fig. 1. If its initial temperature is higher than austenite finish temperature A_f, the whole material is austenite. Suppose that the size of this specimen is L. We may take a representative volume element (RVE) (with volume V and boundary A_0) from it. The size of this RVE is l_1 ($l_1 \ll L$). This RVE consists of many grains. Assume that all grains in this RVE can be divided into N categories according to their grain orientation. Corresponding to a given orientation i, there are M_i grains in this RVE. The volume of jth grain with orientation i is V_{ij} (with boundary A_{ij}), and its size is l_2 ($l_2 \ll l_1$). V_{ij} may transform from pure austenite into a mixture phase of austenite and martensite. For martensite, there are n possible LCVs. Let $k=0$ represent austenite. At one instant, there are Q_{ijk} of type k LCV in V_{ij}. The volume of lth martensite LCV of type k is V_{ijkl} (with boundary A_{ijkl}). In this paper all vectors and tensors are in bold. Summation convention for repeated indices is not used.

Following assumptions are made:

1. The total deformation can be divided into two parts, i.e. elastic deformation and deformation induced by phase transformation.
2. For simplicity, the elastic module ($\mathbf{L}$) of austenite is considered to be the same as that of martensite. Elastic compliance tensor $\mathbf{M}=\mathbf{L}^{-1}$.
3. The distribution of martensite variants in three-dimensional space is random but uniform in every direction.
4. The specific heat C_V of austenite and martensite is the same.
5. The density ρ, temperature field T, heat flow $\mathbf{q}$ are uniform in a RVE.

According to assumption 1, only elastic deformation exists in austenite ($k = 0$)

$$\mathbf{e}_{ij0l} = \mathbf{e}^{\mathrm{e}}_{ij0l} \tag{1}$$

Suppose that the eigenstrain due to phase transformation from austenite (grain orientation i) into type k martensite LCV is $\mathbf{E}^{\mathrm{tr}}_{ik}$. According to assumption 1, the total deformation is the sum of elastic strain $\mathbf{e}^{\mathrm{e}}_{ijkl}$ and phase transformation eigenstrain $\mathbf{E}^{\mathrm{tr}}_{ik}$

$$\mathbf{e}_{ijkl} = \mathbf{e}^{\mathrm{e}}_{ijkl} + \mathbf{E}^{\mathrm{tr}}_{ik} \tag{2}$$

Provided that the specific free energy and specific entropy of austenite and martensite at reference temperature T_0 are u^{A}_0, u^{M}_0, h^{A}_0 and h^{M}_0, respectively. For V_{ijkl} (martensite $k \neq 0$), the specific entropy η^{M}, elastic energy ϕ, and specific internal energy u are

$$\rho\eta^{\mathrm{M}}(T) = h^{\mathrm{M}}_0 + C_V \ln\left(\frac{T}{T_0}\right) \tag{3}$$

$$\phi_{ijkl} = \tfrac{1}{2}(\mathbf{e}_{ijkl} - \mathbf{E}^{\mathrm{tr}}_{ik}) : \mathbf{L} : (\mathbf{e}_{ijkl} - \mathbf{E}^{\mathrm{tr}}_{ik}) = \tfrac{1}{2}\boldsymbol{\sigma}_{ijkl} : \mathbf{M} : \boldsymbol{\sigma}_{ijkl} \tag{4}$$

$$\rho u_{ijkl} = u^{\mathrm{M}}_0 + C_V(T - T_0) + \phi_{ijkl} \tag{5}$$

On the other hand, for V_{ij0l} (austenite $k = 0$), the specific entropy η^{A}, elastic energy ϕ, and specific internal energy u are

$$\rho\eta^{\mathrm{A}}(T) = h^{\mathrm{A}}_0 + C_V \ln\left(\frac{T}{T_0}\right) \tag{6}$$

$$\phi_{ij0l} = \tfrac{1}{2}\mathbf{e}_{ij0l} : \mathbf{L} : \mathbf{e}_{ij0l} = \tfrac{1}{2}\boldsymbol{\sigma}_{ij0l} : \mathbf{M} : \boldsymbol{\sigma}_{ij0l} \tag{7}$$

$$\rho u_{ij0l} = u^{\mathrm{A}}_0 + C_V(T - T_0) + \phi_{ij0l} \tag{8}$$

Hence for a given orientation i, $\mathbf{e}_{ij0l} = 0$ and $\mathbf{e}_{ijkl} = \mathbf{E}^{\mathrm{tr}}_{ik}$ ($k = 1, 2, \ldots, n$) are $n + 1$ potential wells in martensitic transformation.

For any microscopic quantity ψ, its macroscopic quantity may be defined as

$$\langle\psi\rangle = \frac{1}{\rho_t V}\int\int\int_V \rho\psi \,\mathrm{d}V = \frac{1}{\rho_t V}\sum_{i=1}^{N}\sum_{j=1}^{M_i}\sum_{k=0}^{n}\sum_{l=1}^{Q_{ijk}}\int\int\int_{V_{ijkl}} \rho\psi_{ijkl}\,\mathrm{d}V \tag{9}$$

where ρ_t is the macroscopic density of RVE. As volume change is small in phase transformation, the density change due to transformation can be ignored. Hence it is reasonable to assume that density is uniform everywhere, i.e. $\rho = \rho_t$. Recall assumption 5, we then have

$$\langle\psi\rangle = \frac{1}{V}\int\int\int_V \psi \,\mathrm{d}V = \frac{1}{V}\sum_{i=1}^{N}\sum_{j=1}^{M_i}\sum_{k=0}^{n}\sum_{l=1}^{Q_{ijk}}\int\int\int_{V_{ijkl}} \psi_{ijkl}\,\mathrm{d}V \tag{10}$$

Let

$$V_i = \sum_{j=1}^{M_i}\sum_{k=0}^{n}\sum_{l=1}^{Q_{ijk}} V_{ijkl} \tag{11}$$

and

$$c_i = \frac{V_i}{V} \tag{12}$$

Here, c_i is the volume fraction of all crystals with orientation i, and

$$\sum_{i=1}^{N} c_i \equiv 1 \tag{13}$$

For any microscopic quantity ψ, its average along one particular orientation i may be written as

$$\langle \psi \rangle^{(i)} = \frac{1}{V_i} \int\int\int_{V_i} \psi \, \mathrm{d}V = \frac{1}{V_i} \sum_{j=1}^{M_i} \sum_{k=0}^{n} \sum_{l=1}^{Q_{ijk}} \int\int\int_{V_{ijkl}} \psi_{ijkl} \, \mathrm{d}V \tag{14}$$

Note that

$$\langle \psi \rangle = \sum_{i=1}^{N} c_i \langle \psi \rangle^{(i)} \tag{15}$$

For any given orientation i, martensite can be divided into n subgroups according to LCVs. All LCVs of type k form a subgroup (kth group). All austenite make up a subgroup (0th group). Define the volume fraction of kth group along orientation i as

$$z_{ik} = \frac{W_{ik}}{V_i} \tag{16}$$

where

$$W_{ik} = \sum_{j=1}^{M_i} \sum_{l=1}^{Q_{ijk}} V_{ijkl} \tag{17}$$

For any given orientation i,

$$\sum_{k=0}^{n} z_{ik} \equiv 1 \tag{18}$$

The macroscopic volume average strain is defined by

$$\mathbf{E} = \langle \mathbf{e} \rangle \tag{19}$$

From Eq. (2)

$$\mathbf{E} = \mathbf{E}^{\mathrm{e}} + \mathbf{E}^{\mathrm{tr}} \tag{20}$$

where $\mathbf{E}^{\mathrm{e}}$ and $\mathbf{E}^{\mathrm{tr}}$ are macroscopic elastic strain and macroscopic transformation strain, respectively, and

$$\mathbf{E}^{\mathrm{e}} = \langle \mathbf{e}^{\mathrm{e}} \rangle \tag{21}$$

$$\mathbf{E}^{\mathrm{tr}} = \sum_{i=1}^{N} c_i \sum_{k=0}^{n} z_{ik} \mathbf{E}_{ik}^{\mathrm{tr}} \tag{22}$$

Similarly, the macro-average of specific entropy ζ, elastic energy Φ and specific internal energy U can be defined as:

$$\zeta = \langle \eta \rangle \tag{23}$$

$$\Phi = \langle \phi \rangle \tag{24}$$

$$U = \langle u \rangle \tag{25}$$

Substituting Eqs. (3)–(8) into Eqs. (23)–(25) yields

$$\rho\zeta = \langle \rho\eta \rangle = \sum_{i=1}^{N} c_i \left[z_{i0} \left(h_0^{\mathrm{A}} + C_V \ln\left(\frac{T}{T_0}\right)\right) + \sum_{k=1}^{n} z_{ik} \left(h_0^{\mathrm{M}} + C_V \ln\left(\frac{T}{T_0}\right)\right)\right] \tag{26}$$

$$\rho U = \langle \rho u \rangle = \sum_{i=1}^{N} c_i \left[z_{i0} \left(u_0^{\mathrm{A}} + C_V (T - T_0)\right) + \sum_{k=1}^{n} z_{ik} \left(u_0^{\mathrm{M}} + C_V (T - T_0)\right)\right] + \Phi \tag{27}$$

If the macroscopic stress applied on volume V is $\boldsymbol{\Sigma}$, and the surface force applied on its boundary A_0 becomes

$$\mathbf{F} = \boldsymbol{\Sigma} \cdot \mathbf{n} \tag{28}$$

where $\mathbf{n}$ is the normal direction of A_0. It can be proved that

$$\Phi = \langle \phi \rangle = \frac{1}{2} \boldsymbol{\Sigma} : \mathbf{M} : \boldsymbol{\Sigma} + f^{\mathrm{s}} \tag{29}$$

where

$$f^{\mathrm{s}} = \Phi_{\mathrm{int}} = -\frac{1}{2V} \int\int\int_V \boldsymbol{\sigma}_{\mathrm{int}} : \boldsymbol{\varepsilon}^{\mathrm{tr}} \, \mathrm{d}V \tag{30}$$

and

$$\boldsymbol{\varepsilon}^{\mathrm{tr}} = \begin{cases} \mathbf{E}_k^{\mathrm{tr}} & \text{if } \mathbf{x} \in V_{kl} \\ 0 & \text{if } \mathbf{x} \in V_{0l} \end{cases} \tag{31}$$

is eigenstrain of phase transformation, $\boldsymbol{\sigma}_{\mathrm{int}}$ is internal stress field caused by eigenstrain in the absence of external stress field. f^{s}, which may be called ''stored elastic energy'', is the interaction energy due to internal stress field $\boldsymbol{\sigma}_{\mathrm{int}}$. It can be proved that f^{s} does not directly depend on external stress field $\boldsymbol{\Sigma}$, but only relates to the microscopic structure of martensite and the distribution of martensite variant. Following internal variable theory (Coleman and Gutin, 1967), it is reasonable to assume that the behavior of a SMA only depends on the current volume fractions of martensite LCVs. In general,

$$f^{\mathrm{s}} = f^{\mathrm{s}}(c_1, c_2, \ldots, c_N,\ z_{11}, z_{12}, \ldots, z_{1n},\ \ldots,\ z_{i1}, z_{i2}, \ldots, z_{in},\ \ldots,\ z_{N1}, z_{N2}, \ldots, z_{Nn}) \tag{32}$$

Let

$$f_i^{\mathrm{s}} = -\frac{1}{2V_i} \int\int\int_{V_i} \boldsymbol{\sigma}_{\mathrm{int}} : \boldsymbol{\varepsilon}^{\mathrm{tr}} \, \mathrm{d}V \tag{33}$$

From Eqs. (15), (30) and (33)

$$f^{\mathrm{s}} = \sum_{i=1}^{N} c_i f_i^{\mathrm{s}} \tag{34}$$

For simplicity, the coupling effect between different orientation may be ignored, and only the interaction between same orientation group is taken into consideration. Hence,

$$f_i^{\mathrm{s}} = f_i^{\mathrm{s}}(z_{i1}, z_{i2}, \ldots, z_{in}) \tag{35}$$

Furthermore, it can be proved that f_i^{s} is a second order polynomial function of volume fraction. In general, f_i^{s} can be written as

$$f_i^{\mathrm{s}} = Az_{i0}(1 - z_{i0}) + \frac{1}{2}\sum_{k=1}^{n}\sum_{\substack{l=1\\ l\neq k}}^{n} B_{kl} z_{ik} z_{il} \tag{36}$$

where A and B_{kl} are materials constants, which only depend upon phase transformation eigenstrain. Due to symmetry of martensite variants, it can also be proved that the number of coefficients B_{kl} is less than n. In practice, A and B_{kl} may be measured from macroscopic experiment as mentioned later. In previous models (for instance, Goo and Lexcellent, 1997; Huang and Brinson, 1998; Patoor et al., 1995, 1998; Gall and Sehitoglu, 1999), Eshelby inclusion theory are applied to estimate the interaction energy among HPVs. As mentioned above, in martensitic transformation, LCVs instead of HPVs are potential wells. Thus, the interaction energy should be expressed as volume fraction of LVCs rather than HPVs. On the other hand, it is well known that martensite variants are polyhedron as habit plane and twin plane are plane. Eshelby inclusion theory which provides a nice closed form solution for interaction energy of elliptical inclusion may not produce good estimation for SMAs.

In Eq. (36), the first term represents the interphase (between austenite and martensite) energy stored in habit plane, and the second term stands for the elastic distortion energy stored in the interface of twinned martensite. Rogers (1996) discussed the interaction energy between two martensite variants by means of non-local interaction method. It is well known that habit plane between austenite and martensite is not full-coherent interface, while twinning plane between martensite variants are coherent interface. As pointed out by Seelecke (1996), stored energy in twinning plane is smaller than interface energy between habit plane at least by one magnitude order. By ignoring second term, Eq. (36) may be written as

$$f_i^{\mathrm{s}} = Az_{i0}(1 - z_{i0}) \tag{37}$$

From Eqs. (34) and (37)

$$f^{\mathrm{s}} = \sum_{i=1}^{N} c_i f_i^{\mathrm{s}} = \sum_{i=1}^{N} c_i A z_{i0}(1 - z_{i0}) \tag{38}$$

From Eqs. (29) and (34)

$$\Phi = \frac{1}{2}\boldsymbol{\Sigma} : \mathbf{M} : \boldsymbol{\Sigma} + \sum_{i=0}^{N} c_i f_i^{\mathrm{s}} \tag{39}$$

Thus

$$\rho U = \frac{1}{2}\boldsymbol{\Sigma} : \mathbf{M} : \boldsymbol{\Sigma} + \sum_{i=1}^{N} c_i \left[z_{i0}\left(u_0^{\mathrm{A}} + C_V(T - T_0)\right) + \sum_{k=1}^{n} z_{ik}\left(u_0^{\mathrm{M}} + C_V(T - T_0)\right) + f_i^{\mathrm{s}} \right] \tag{40}$$

and

$$\begin{aligned} \frac{1}{V}\int\int_{A_0} \mathbf{F}\cdot\mathbf{u}\,\mathrm{d}A &= \frac{1}{V}\int\int_{A_0} \mathbf{n}\cdot\boldsymbol{\Sigma}\cdot\mathbf{u}\,\mathrm{d}A = \frac{1}{V}\boldsymbol{\Sigma} : \int\int_{A_0} \mathbf{n}\otimes\mathbf{u}\,\mathrm{d}A = \frac{1}{V}\boldsymbol{\Sigma} : \int\int\int_{V} \mathbf{e}\,\mathrm{d}V = \boldsymbol{\Sigma} : \langle\mathbf{e}\rangle \\ &= \boldsymbol{\Sigma} : \mathbf{E} \end{aligned} \tag{41}$$

The Gibbs free energy function becomes

$$\begin{aligned}\rho G &= \rho U - T\rho\zeta - \boldsymbol{\Sigma} : \mathbf{E} \\ &= \rho U - T\rho\zeta - \boldsymbol{\Sigma} : \left(\mathbf{E}^{\mathrm{e}} + \sum_{i=1}^{N} c_i \sum_{k=0}^{n} z_{ik} \mathbf{E}_{ik}^{\mathrm{tr}} \right) \\ &= \rho U - T\rho\zeta - \boldsymbol{\Sigma} : \mathbf{M} : \boldsymbol{\Sigma} - \boldsymbol{\Sigma} : \left(\sum_{i=1}^{N} c_i \sum_{k=0}^{n} z_{ik} \mathbf{E}_{ik}^{\mathrm{tr}} \right) \\ &= \sum_{i=1}^{N} c_i \left[z_{i0} \left(u_0^{\mathrm{A}} + C_V (T - T_0) \right) + \sum_{k=1}^{n} z_{ik} \left(u_0^{\mathrm{M}} + C_V (T - T_0) \right) + f_i^{\mathrm{s}} \right] \\ &\quad - T \left\{ \sum_{i=1}^{N} c_i z_{i0} \left(h_0^{\mathrm{A}} + C_V \ln \left(\frac{T}{T_0} \right) \right) \right. \\ &\quad \left. + \sum_{k=1}^{n} z_{ik} \left(h_0^{\mathrm{M}} + C_V \ln \left(\frac{T}{T_0} \right) \right) \right\} - \boldsymbol{\Sigma} : \left(\sum_{i=1}^{N} c_i \sum_{k=0}^{n} z_{ik} \mathbf{E}_{ik}^{\mathrm{tr}} \right) - \frac{1}{2} \boldsymbol{\Sigma} : \mathbf{M} : \boldsymbol{\Sigma} \end{aligned} \tag{42}$$

According to the internal variable theory,

$$\mathbf{E} = -\rho \frac{\partial G}{\partial \boldsymbol{\Sigma}} = \mathbf{M} : \boldsymbol{\Sigma} + \sum_{i=1}^{N} c_i \sum_{k=0}^{n} z_{ik} \mathbf{E}_{ik}^{\mathrm{tr}} \tag{43}$$

Let Ξ_{ik} be the thermodynamic driving force corresponding to internal variable z_{ik}

$$\Xi_{ik} = -\rho \frac{\partial G}{\partial z_{ik}} = \boldsymbol{\Sigma} : \mathbf{E}_{ik}^{\mathrm{tr}} + (\Delta h T - \Delta u) - \frac{\partial f_i^{\mathrm{s}}}{\partial z_{ik}} \tag{44}$$

where

$$\left. \begin{aligned} \Delta h &= h_0^{\mathrm{M}} - h_0^{\mathrm{A}} \\ \Delta u &= u_0^{\mathrm{M}} - u_0^{\mathrm{A}} \end{aligned} \right\} \tag{45}$$

It has been demonstrated by experiments (Huo and Müller, 1993) that both Δh and Δu are negative. Since $T^{\mathrm{eq}} = \frac{\Delta u}{\Delta h}$ is phase equilibrium temperature, $\Delta u = \Delta h T^{\mathrm{eq}}$ is latent heat upon phase change. Let $\rho\eta^*$ be local entropy production due to microstructure rearrangement, the strong form of the second thermodynamic law may be expressed as

$$\rho T \eta^* = \sum_{i=1}^{N} c_i \sum_{k=1}^{n} \Xi_{ik} \dot{z}_{ik} - \frac{1}{T} \mathbf{q} \cdot \nabla T \geqslant 0 \tag{46}$$

Substitution of Eq. (38) into Eq. (44) results in

$$\Xi_{ik} = \boldsymbol{\Sigma} : \mathbf{E}_{ik}^{\mathrm{tr}} + (\Delta h T - \Delta u) + A(1 - 2z_{i0}) \tag{47}$$

As mentioned above, polycrystalline material can be considered at two different levels. At the first level, we consider the grains whose austenite has the same orientation as one group. Grains belonging to the same group (as shown by the gray areas in Fig. 1) need not be distinguished, and their macroscopic effect only depends on their volume fraction c_i in RVE. At the second level, in each group with the same orientation, $n + 1$ subgroups can be classified, i.e. n different martensite LCVs plus one for austenite. Different martensite variants in the same subgroup (as shown by black areas in Fig. 1) need not be distinguished, and their macroscopic effect is only determined by their volume fraction, which can be described by f_i^{s}. In the case where only one martensite variant is produced in the transformation, if internal friction can be ignored, then constant A represents the magnitude of hysteresis in strain vs. stress curve in an isothermal loading/unloading test (see Fig. 2). In trilinear model (Abeyaratne and Knowles, 1993; Huo and Müller,

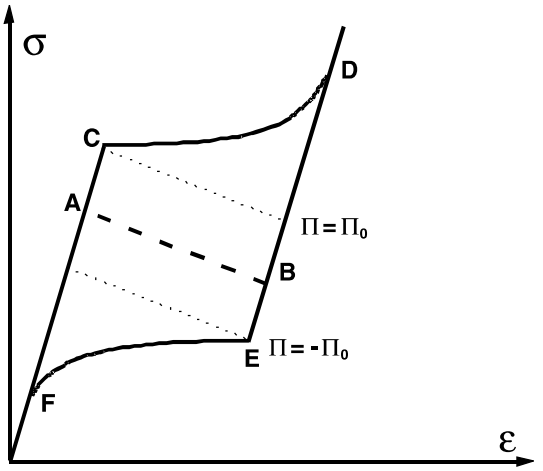

Fig. 2. The critical condition for nucleation and evolution in phase transformation.

1993), constant A is proportional to the slope of second line (refer to Fig. 3 of Abeyaratne and Knowles, 1993; Figs. 4 and 20 of Huo and Müller, 1993). Thus constant A can be measured from tensile test of single variant phase transformation.

As mentioned above, LCVs are potential wells instead of HPVs. That is to say, in forward phase transformation, austenite transfers into HPV instead of transition into LCV directly; in reverse transformation, HPV instead of LCV changes back into austenite. Therefore, the relationship between HPV and LCV must be provided. For any given orientation i, introducing volume fraction z_{il}^* for H possible HPVs, which has a direct relation with volume fraction of LCVs as

$$z_{ik} = \sum_{l=1}^{H} v_{kl} z_{il}^* \quad (k = 0, 1, 2, \ldots, n) \tag{48}$$

where v_{kl} is stoichiometric coefficient related to volume fraction of HPV z_{il}^*. For any given orientation the following equation is satisfied

$$\sum_{k=0}^{n} v_{kl} = 0 \tag{49}$$

The stoichiometric coefficient v_{kl} does not vary with orientation, and it is the same as the stoichiometric coefficient in single crystal. H, which equals to the total number of HPVs in single crystal SMA, does not vary with orientation as well. v_{kl} and H are solely determined by the crystal structures of austenite and martensite.

The phase transformation eigenstrain related to volume fraction z_{il}^* of HPV is

$$\mathbf{E}_{il}^* = \sum_{k=1}^{n} v_{kl} \mathbf{E}_{ik}^{\mathrm{tr}} \tag{50}$$

The thermodynamic driving force corresponding to z_{il}^* is

$$\Pi_{il} = \boldsymbol{\Sigma} : \mathbf{E}_{il}^* + (\Delta hT - \Delta u) + A(1 - 2z_0) \tag{51}$$

The second thermodynamic principle may be written as

$$\rho T\eta^* = \sum_{i=1}^{N} c_i \sum_{l=1}^{H} \Pi_{il}\dot{z}_{il}^* - \frac{1}{T}\mathbf{q}\cdot\nabla T \geqslant 0 \tag{52}$$

From previous experimental results in the literature (such as Huo and Müller, 1993), the critical condition for phase transformation start may be expressed as,

$$\Pi_{il} = \Pi_{il}^{c\pm}, \quad (l = 1, 2, \ldots, H) \tag{53}$$

where "+" corresponds to the forward transformation, and "−" corresponds to the reverse transformation. $\Pi_{il}^{c+} > 0$ and $\Pi_{il}^{c-} < 0$ correspond to the critical thermodynamic driving forces for forward transformation and reverse transformation, respectively.

On the other hand, the evolution equation for phase transformation may be expressed as

$$\left.\begin{aligned} \dot{\Pi}_{il} &= \dot{\Pi}_{il}^{c+} = 2\left(\lambda + \mu\tfrac{1}{z_{i0}}\right)\dot{z}_{il}^* \quad \text{for forward transformation} \\ \dot{\Pi}_{il} &= \dot{\Pi}_{il}^{c-} = 2\left(\lambda + \mu\tfrac{1}{z_{il}^*}\right)\dot{z}_{il}^* \quad \text{for reverse transformation} \end{aligned}\right\} \tag{54}$$

Here, μ is introduced to describe hardening behavior. In forward transformation, Π_{il}^{c+} increases, while in reverse transformation, Π_{il}^{c-} decreases. As soon as nucleation starts in forward transformation, Π_{il}^{c-} moves back to its maximum value $(-\Pi_0)$. When reverse transformation starts, Π_{il}^{c+} returns back to its minimum value (Π_0). Here, Π_0, λ and μ are non-negative material constants. As shown in Fig. 2, it is apparent that the sum of $A + \Pi_0$ represents the hysteresis in phase transformation, where A is produced by the energy on the interphase between austenite and martensite, and Π_0 is due to internal–friction in phase transformation. Lexcellent et al. (1996) and others take $A = 0$, so hysteresis is considered to be only the result of internal-friction in phase transformation. On the other hand, Huo and Müller (1993) considered $\Pi_0 = 0$, i.e. the hysteresis is due to interphase energy only. Thus, point A is coincident with point C, and point B superposes with point E. If $\mu = 0$, $(\lambda - A)$ is proportional to the slope of $\overline{\mathrm{CD}}$. Whether the material appears to be hardening or softening depends on $(\lambda - A)$ rather than only $(-A)$. This conclusion is different from Goo and Lexcellent (1997) and others. The real phase transformation path is along non-equilibrium path $\overline{\mathrm{CD}}$ instead of equilibrium path $\overline{\mathrm{AB}}$. It means that the entropy is always increased with the phase transformation progressing. For a material with harden behavior, we usually have relation

$$\lambda > A \tag{55}$$

If $\Pi_0 = 0$ and $\lambda = \mu = 0$, Eqs. (53) and (54) result in the same form as trilinear model. In general, $\mu \ll \lambda$. So at the beginning of phase transformation, evolution curve CD is almost a straight line. When phase transformation are nearly completed, z_{i0} is close to 0. First formula in Eq. (54) can be approximately written as $\dot{\Pi}_{il} = \dot{\Pi}_{il}^{c+} = \frac{2\mu}{z_{i0}}\dot{z}_{il}^*$. It is similar to Tanaka's model (Tanaka et al., 1994). From Eq. (54), for forward transformation

$$\Pi_{il}\dot{z}_{il}^* = \frac{z_{i0}}{2(\lambda z_{i0} + \mu)}\Pi_{il}\dot{\Pi}_{il} = \frac{z_{i0}}{4(\lambda z_{i0} + \mu)}\frac{\mathrm{d}}{\mathrm{d}t}(\Pi_{il}^{c+})^2 \geqslant 0 \tag{56}$$

while for reverse transformation

$$\Pi_{il}\dot{z}_{il}^* = \frac{z_{il}^*}{2(\lambda z_{il}^* + \mu)}\Pi_{il}\dot{\Pi}_{il} = \frac{z_{il}^*}{4(\lambda z_{il}^* + \mu)}\frac{\mathrm{d}}{\mathrm{d}t}(\Pi_{il}^{c-})^2 \geqslant 0 \tag{57}$$

So Eq. (52) can always be satisfied.

From Eqs. (53) and (54), we can get volume fraction of each HPV. Subsequently, eigenstrain of phase transformation can be solved from Eqs. (48) and (22). Substituting Eq. (48) into Eq. (22) and combining with Eq. (50) yield

$$\mathbf{E}^{\mathrm{tr}} = \sum_{i=1}^{N} c_i \sum_{k=0}^{n} \sum_{l=1}^{H} v_{kl} z_{il}^{*} \mathbf{E}_{ik}^{\mathrm{tr}} = \sum_{i=1}^{N} c_i \sum_{l=1}^{H} z_{il}^{*} \left(\sum_{k=0}^{n} v_{kl} \mathbf{E}_{ik}^{\mathrm{tr}} \right) = \sum_{i=1}^{N} c_i \sum_{l=1}^{H} z_{il}^{*} \mathbf{E}_{il}^{*} \tag{58}$$

i.e.,

$$\mathbf{E}^{\mathrm{tr}} = \sum_{i=1}^{N} c_i \sum_{l=1}^{H} z_{il}^{*} \mathbf{E}_{il}^{*} \tag{59}$$

Provided that the unit normal vector of habit plane is $\mathbf{n}_{il}$, the phase transformation eigenstrain can be written as

$$\mathbf{C}_{il} = (\mathbf{I} + \mathbf{n}_{il} \otimes \mathbf{b}_{il})(\mathbf{I} + \mathbf{b}_{il} \otimes \mathbf{n}_{il}) \tag{60}$$

Thus

$$\mathbf{E}_{il}^{*} = \tfrac{1}{2}[\mathbf{C}_{il} - \mathbf{I}] = \tfrac{1}{2}[(\mathbf{n}_{il} \otimes \mathbf{b}_{il} + \mathbf{b}_{il} \otimes \mathbf{n}_{il}) + \mathbf{b}_{il}^{2}(\mathbf{n}_{il} \otimes \mathbf{n}_{il})] \tag{61}$$

Generally speaking, transformation eigenstrain includes not only shear deformation, but also a small amount of volume change. Therefore, $\mathbf{b}_{il}$ is normally not perpendicular to $\mathbf{n}_{il}$. Decompose vector $\mathbf{b}_{il}$ into two parts (Fig. 3): one is in $\mathbf{n}_{il}$ direction, and the other is vertical to $\mathbf{n}_{il}$

$$\mathbf{b}_{il} = g\mathbf{m}_{il} + \varepsilon_0 \mathbf{n}_{il} \tag{62}$$

where, g is the magnitude of shear deformation, and ε_0 is strain due to volume change. Hence

$$\mathbf{E}_{il}^{*} = g\mathbf{P}_{il} + \varepsilon \mathbf{n}_{il} \otimes \mathbf{n}_{il} \tag{63}$$

where

$$\mathbf{P}_{il} = \tfrac{1}{2}(\mathbf{m}_{il} \otimes \mathbf{n}_{il} + \mathbf{n}_{il} \otimes \mathbf{m}_{il}) \tag{64}$$

and

$$\varepsilon = \varepsilon_0 + \tfrac{1}{2}\left(g^2 + \varepsilon_0^2\right) \tag{65}$$

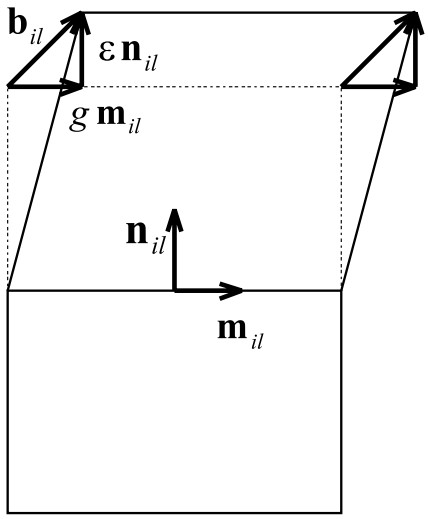

Fig. 3. Eigenstrain in phase transformation in HPV: $\mathbf{b}_{il} = g\mathbf{m}_{il} + \varepsilon \mathbf{n}_{il}$.

By substituting Eq. (61) into Eq. (51)

$$\Pi_{il} = \tau_{il} g - \Theta_{il}\varepsilon + (\Delta hT - \Delta u) + A(1 - 2z_0) \tag{66}$$

where

$$\tau_{il} = \mathbf{\Sigma} : \mathbf{P}_{il} \tag{67}$$

which is the resolved shear stress, and

$$\Theta_{il} = -\mathbf{n}_{il} \cdot \mathbf{\Sigma} \cdot \mathbf{n}_{il} \tag{68}$$

is the equivalent pressure. So $\Theta_{il}\varepsilon$ represents the effect of asymmetry of thermodynamic driving force for phase transformation in tension and compression.

3. Simplified model

In the previous section, a thermodynamical constitutive model for polycrystalline SMAs under any loading condition is established. For further simplification, following assumptions are applied,

(a) A polycrystalline SMA includes a lot of randomly but uniformly distributed grains, and the material is isotropic. So we can suppose that N orientation groups are uniformly distributed. Thus, the volume fraction of each orientation group is the same, i.e. $c_i = \frac{1}{N} (i = 1, 2, \ldots, N)$.

(b) The interaction between different HPVs is ignored, i.e. $\mu = 0$ in Eq. (54). And suppose that the mechanism of phase transformation is the same as that in single variant phase transformation. So each orientation group has H possible phase transformation systems, and they are independent on each other.

From assumptions (a) and (b), we may directly divide a RVE into R orientation components, where $R = N \times H$. The volume fraction of each orientation component in this RVE is $1/R$, and the transformation mechanism of each orientation component is the same as that in single variant phase transformation.

(c) The volume change in phase transformation is ignored, i.e. $\varepsilon = 0$ in Eq. (63).

From above assumptions, a RVE consists of R orientation components. Let martensite volume fraction of orientation component k be z_k, then the volume fraction of austenite is $z_{k0} = 1 - z_k$, Eq. (59) becomes

$$\mathbf{E}^{\mathrm{tr}} = \frac{1}{R} g \sum_{k=1}^{R} z_k \mathbf{P}_k \tag{69}$$

where

$$\mathbf{P}_k = \tfrac{1}{2}(\mathbf{m}_k \otimes \mathbf{n}_k + \mathbf{n}_k \otimes \mathbf{m}_k) \tag{70}$$

Here, $\mathbf{n}_k$ and $\mathbf{m}_k$ are distributed uniformly on a unit spherical surface.

Resolve shear stress as

$$\tau_k = \mathbf{\Sigma} : \mathbf{P}_k \tag{71}$$

Then Eq. (66) may be written as

$$\Pi_k = \tau_k g + (\Delta hT - \Delta u) - A(1 - 2z_k) \tag{72}$$

The critical condition for phase transformation start becomes,

$$\Pi_k = \Pi_k^{\mathrm{c}\pm}, \quad (k = 1, 2, \ldots, R) \tag{73}$$

And the equation for evolution of phase transformation becomes

$$\left.\begin{array}{ll}\dot{\boldsymbol{\Pi}}_k = \dot{\boldsymbol{\Pi}}_k^{c+} = 2\lambda\dot{z}_k^* & \text{for forward transformation} \\ \dot{\boldsymbol{\Pi}}_k = \dot{\boldsymbol{\Pi}}_k^{c-} = 2\lambda\dot{z}_k^* & \text{for reverse transformation}\end{array}\right\} \tag{74}$$

As long as the martensite volume fraction of each orientation component is determined, the total strain can be calculated by

$$\mathbf{E} = \mathbf{M} : \boldsymbol{\Sigma} + \frac{1}{R} g \sum_{k=1}^{R} z_k \mathbf{P}_k \tag{75}$$

4. Numerical simulation

In this section, numerical simulation of a Cu–Al–Zn–Mn polycrystalline SMA round tube is presented. The simplified model proposed above is used to simulate the mechanical behavior of this tube. The numerical simulation is based on the experiments reported by Sittner et al. (1995). The thin wall specimen for the experiments were made of Cu–10Al–5Zn–5Mn (wt.%) polycrystalline SMA produced by Fulrukawa Co. with external diameter $d_{\text{ext}} = 8$ mm, and internal diameter $d_{\text{int}} = 5$ mm. The specimens were finally heat treated at 873 K for 2 h and quenched in ice water. The measured grain size $d \leqslant 120$ μm. Transformation temperatures were obtained by electric resistivity measurements. The main material parameters of this tube is listed in Table 1 (refer to Fig. 1 in Sittner et al. (1995) for details). A Shimadzu AG-10TS testing machine designed for combined tension–torsion tests with a closed loop servo-control analog system was adapted for simultaneously applied cycle tension and torsion in force or strain control using PC. A special combined strain extensometer was calibrated to avoid cross effects among tension and torsion in the interval of used extensions and angles of rotation. Combined tension and torsion load tests were performed at room temperature $T = 285$ K in strain or force control mode. Since ambient temperature is higher than austinite finish temperature A_f of the specimen, it was pseudoelastic deformation under tension plus torsion loads.

Sittner et al. (1995) introduced new definitions for equivalent shear stress τ and equivalent shear strain γ. The relationship between equivalent shear stress τ and the engineering shear stress τ_{real}, and the relationship between equivalent shear γ and engineering shear strain γ_{real} are,

$$\tau = c^s \tau_{\text{real}} \tag{76}$$

$$\gamma = \gamma_{\text{real}} / c^e \tag{77}$$

where

$$c^s = 1.23 \tag{78}$$

$$c^e = 2.21 \tag{79}$$

In order to compare the simulation results with the measurements in Sittner et al. (1995), the equivalent shear stress and equivalent shear strain reported by Sittner et al. (1995) are used. Two types of experiments were reported by Sittner et al. (1995). In the first type, it was strain control. Corresponding to the controlled "strain path" (ε, γ), the evolution of the resulting stress (σ, τ) were measured which are called as

Table 1
Parameters for Cu–Al–Zn–Mn reported in Sittner et al. (1995)

E_0 (GPa)	G_0 (GPa)	T (K)	M_s (K)	M_f (K)	A_s (K)	A_f (K)
53.0	19.5	285	239	223	248	260

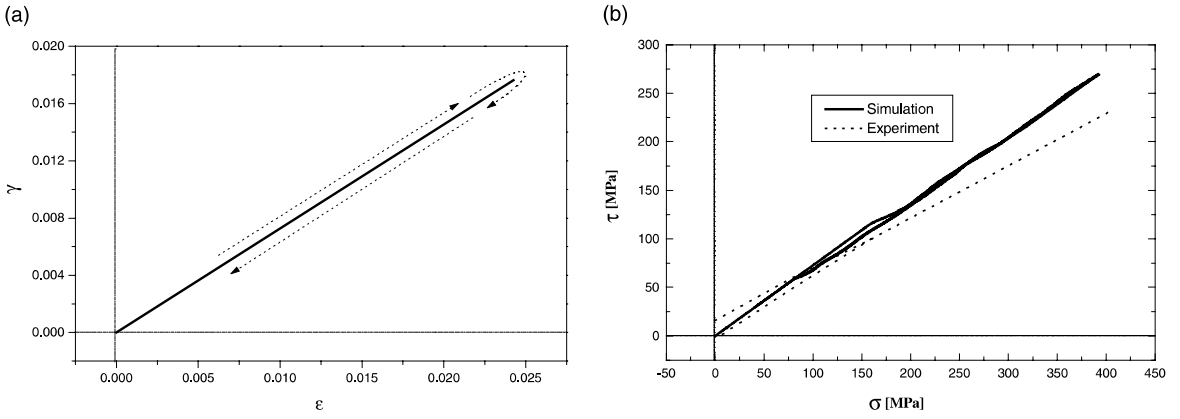

Fig. 4. (a) Imposed strain path and (b) stress path.

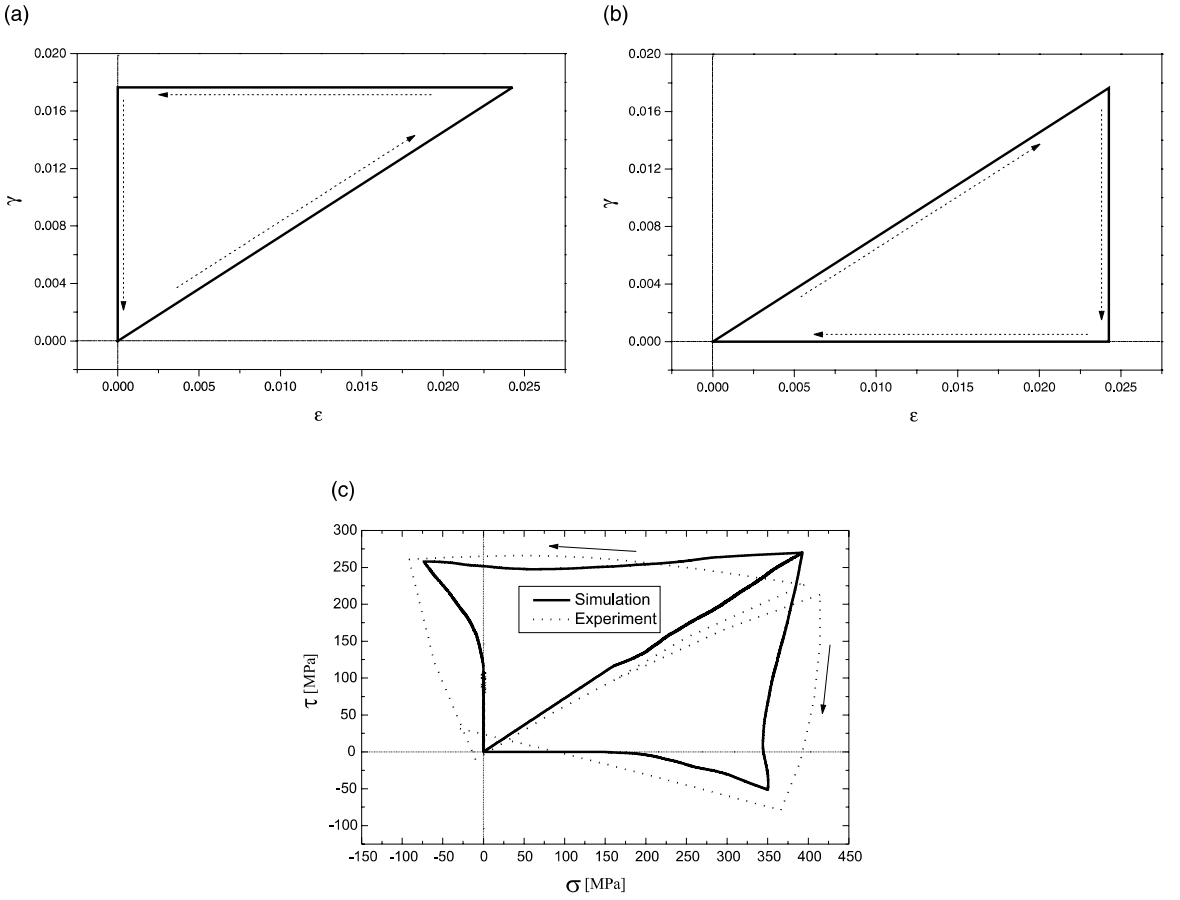

Fig. 5. (a) Imposed strain path, (b) imposed strain path and (c) stress path.

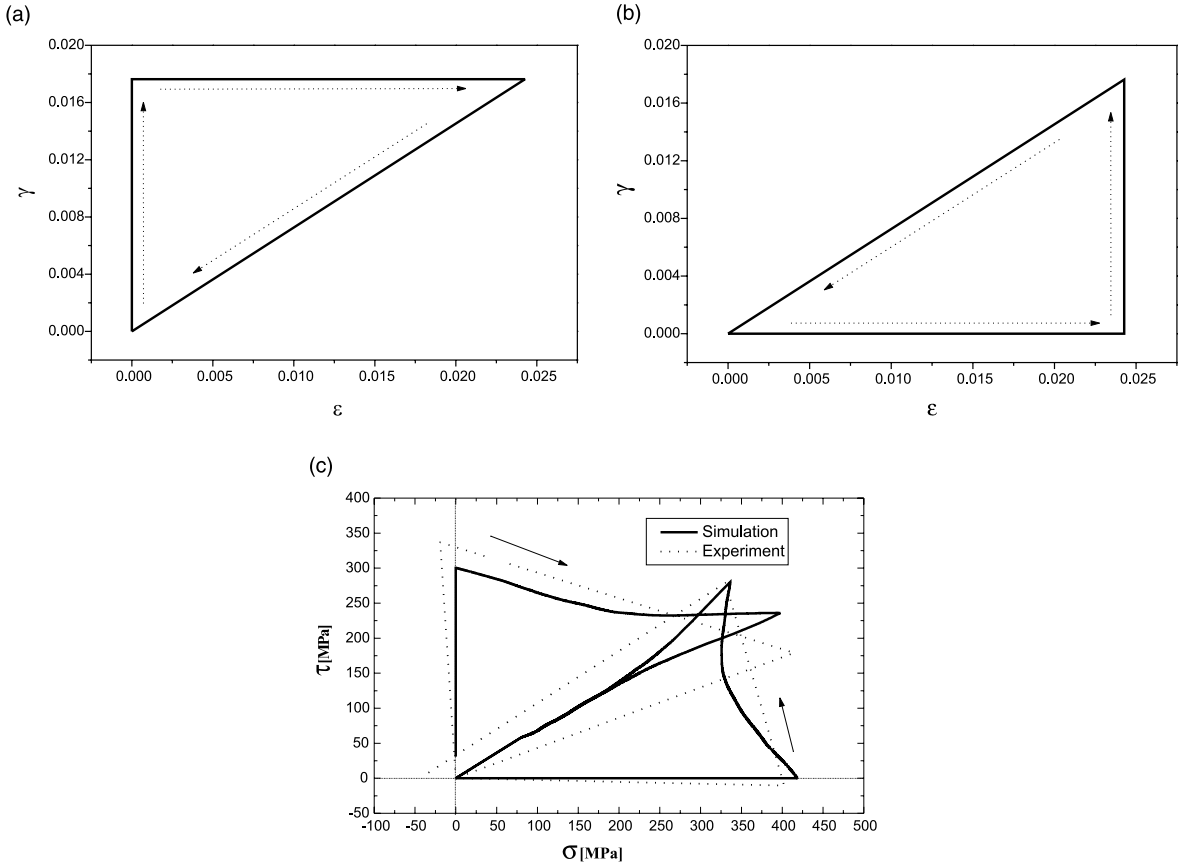

Fig. 6. (a) Imposed strain path, (b) imposed strain path and (c) stress path.

"corresponding stress path". In the other type, the control parameter was stress. The corresponding strains which are called as the "corresponding strain path" were measured.

In order to use the proposed model, following parameters have to be determined:

(1) The shape change parameters in martensitic transformation, g, ε: In simplified orientation component model, $\varepsilon = 0$. g can be calibrated directly from the magnitude of macroscopic deformation in experiment as explained later.

(2) Mechanics parameter, $\mathbf{L}$: The elastic constants of austenite and martensite are the same. The values of elastic modulus and shear modulus are listed in Table 1.

(3) Thermodynamic parameters: Δh, Δu, A, Π_0, λ, A_s, A_f, M_s, M_f, T^{eq}.

Provided that a single crystal specimen is stretched under a uni-axial load. The direction of load is carefully chosen, so only one particular martensite HPV, which is favorable by applied stress, is produced. Suppose that the normal direction of habit plane of this HPV is $\mathbf{n}$, and the shear direction is $\mathbf{m}$, then loading direction is along $(\sqrt{2}/2)(\mathbf{n}+\mathbf{m})$. Hence we have the maximum transformation strain $\varepsilon_0 = (1/2)g$. For Cu–Zn–Al–Mn, ε_0 is estimated as 0.16 from Fig. 2(a) of Sittner et al. (1995). Eq. (72) becomes

$$\Pi = \sigma \cdot \varepsilon_0 + T\Delta h - \Delta u - A(1-2z) \tag{80}$$

The austenite and martensite start/finish temperature A_s, A_f, M_s, M_f and room temperature T are shown in Table 1.

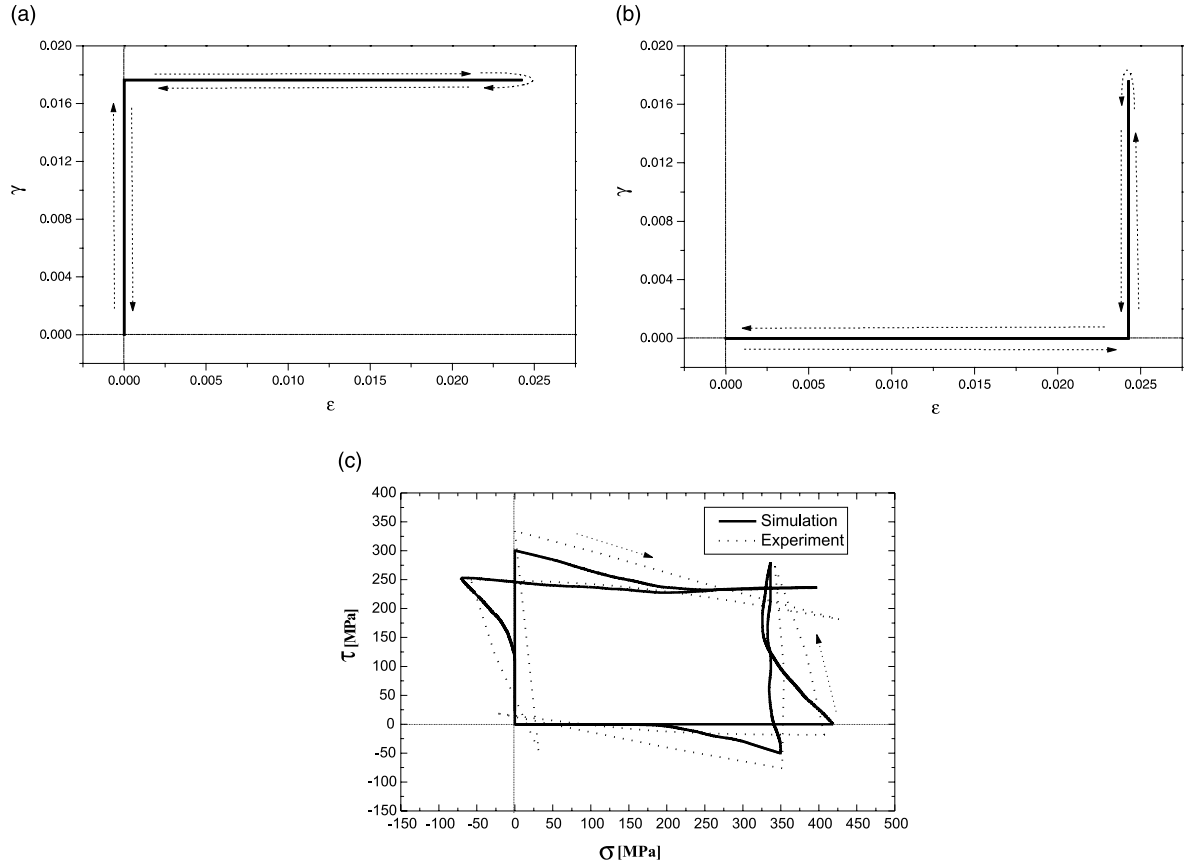

Fig. 7. (a) Imposed strain path, (b) imposed strain path and (c) stress path.

Stress free state gives $\sigma = 0$. If the material is austenite (i.e. $z = 0$) and temperature equals to martensite start temperature (i.e. $T = M_s$), then $\Pi = \Pi_0$. If the material is martensite (i.e. $z = 1$) and temperature equal to austenite start temperature (i.e. $T = A_s$), then $\Pi = -\Pi_0$. Substituting them into Eq. (80) we obtain

$$\left.\begin{aligned} M_s \Delta h - \Delta u - A &= \Pi_0 \\ A_s \Delta h - \Delta u + A &= -\Pi_0 \end{aligned}\right\} \tag{81}$$

From Eq. (81) and the definition of T^{eq} we obtain

$$T^{eq} = \frac{\Delta u}{\Delta h} = \frac{1}{2}(A_s + M_s) \tag{82}$$

Suppose that at $\sigma = \sigma_1$ the martensite start temperature is T_1, while at $\sigma = \sigma_2$ the martensite start temperature is T_2. Substituting them into Eq. (80) and taking subtraction, we obtain

$$\Delta h = -\frac{(\sigma_2 - \sigma_1)}{(T_2 - T_1)}\varepsilon_0 \tag{83}$$

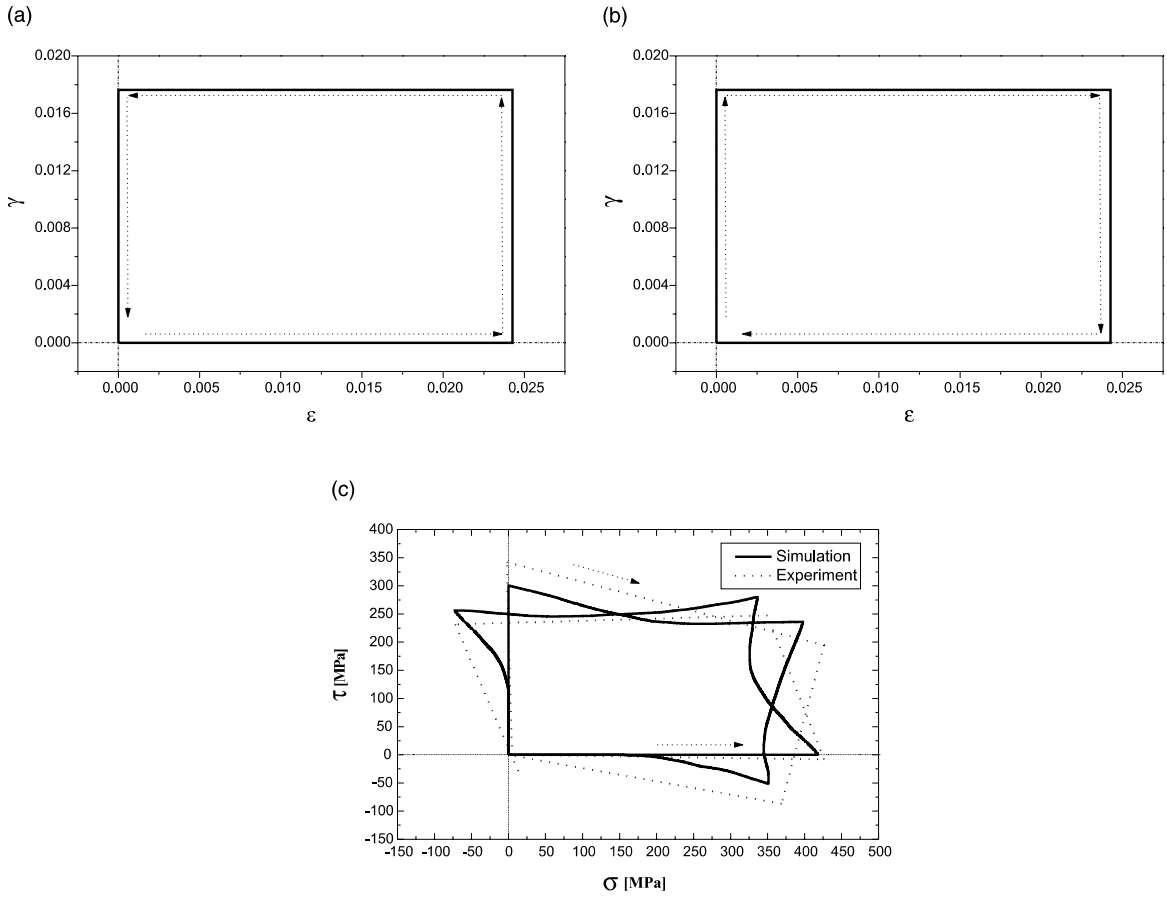

Fig. 8. (a) Imposed strain path, (b) imposed strain path and (c) stress path.

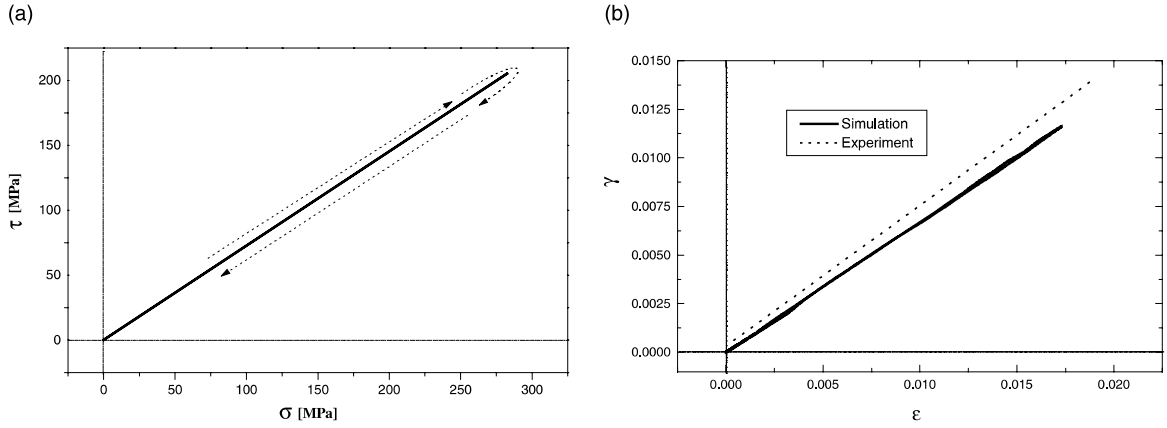

Fig. 9. (a) Imposed stress path and (b) strain path.

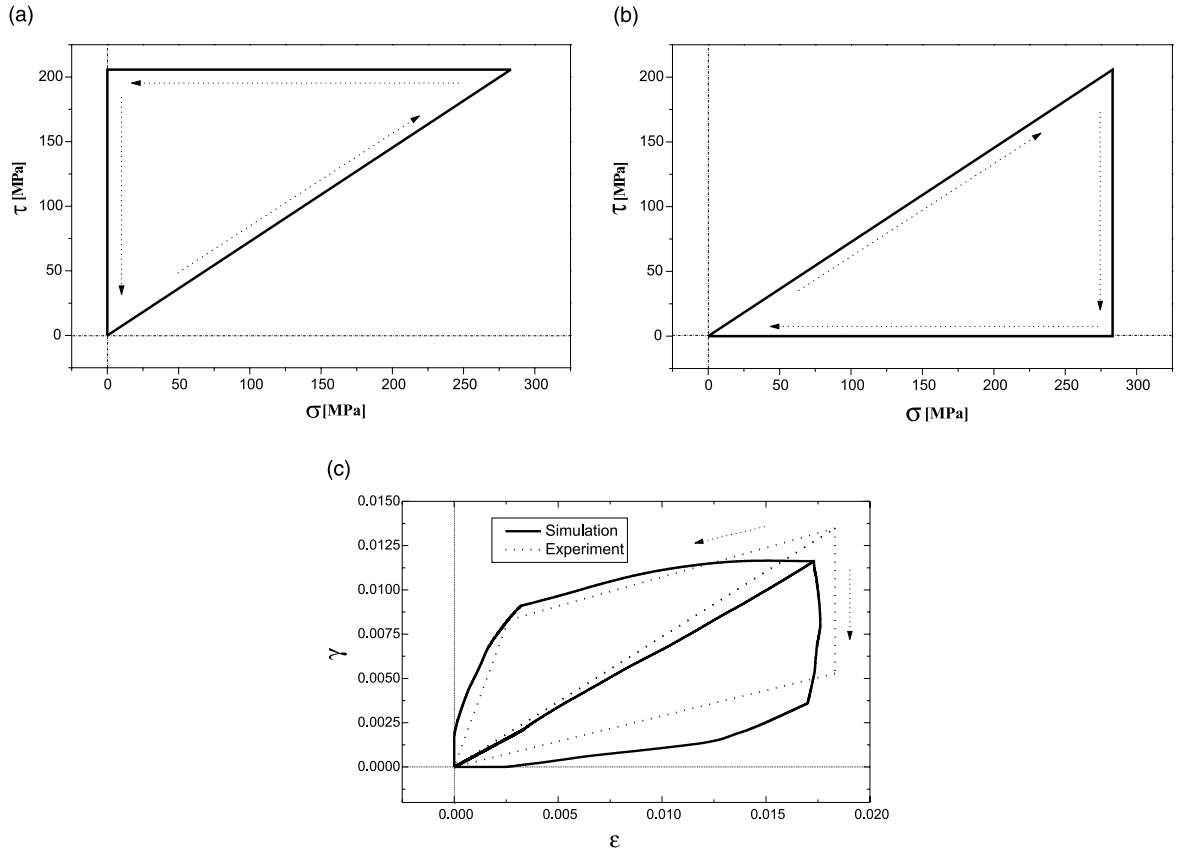

Fig. 10. (a) Imposed stress path, (b) imposed stress path and (c) strain path.

From Eqs. (82) and (83)

$$\Delta u = T^{\mathrm{eq}}\Delta h = -\frac{(A_{\mathrm{s}} + M_{\mathrm{s}})(\sigma_2 - \sigma_1)}{2(T_2 - T_1)}\varepsilon_0 \tag{84}$$

From Eq. (81)

$$A + \Pi_0 = -\frac{(A_{\mathrm{s}} - M_{\mathrm{s}})}{2}\Delta h = \frac{(A_{\mathrm{s}} - M_{\mathrm{s}})(\sigma_2 - \sigma_1)}{2(T_2 - T_1)}\varepsilon_0 \tag{85}$$

From Eq. (85), $A + \Pi_0$ can be determined. But the exact portions of A and Π_0 depend on the material. Roughly

$$\left.\begin{aligned} A &= k_0 \tfrac{(A_{\mathrm{s}} - M_{\mathrm{s}})(\sigma_2 - \sigma_1)}{2(T_2 - T_1)}\varepsilon_0 \\ \Pi_0 &= (1 - k_0)\tfrac{(A_{\mathrm{s}} - M_{\mathrm{s}})(\sigma_2 - \sigma_1)}{2(T_2 - T_1)}\varepsilon_0 \end{aligned}\right\} \tag{86}$$

where $0 \leqslant k_0 \leqslant 1$. In fact, the value of A can be determined by experiment in which single martensite variant is induced (see Section 4.3 in Huo and Müller, 1993 for details). As shown in Fig. 2, If the phase equilibrium path $\overline{\mathrm{AB}}$ is obtained in uniaxial tension test in which single martensite variant is induced

$$A = \frac{(\sigma_A - \sigma_B)\varepsilon_0^2}{2\varepsilon_B^{tr}} \tag{87}$$

where ε_B^{tr} is phase transformation strain at point B, which equals to total strain subtracted by elastic strain

$$\varepsilon_B^{tr} = \varepsilon_B - \varepsilon_B^e = \varepsilon_B - \frac{\sigma_B}{E} \tag{88}$$

Numerical simulation shows that the effect of the variation of k_0 in polycrystalline SMA is small. In the absence of experimental result in which single martensite variant is induced, here we take k_0 as 0.1.

By substituting Eq. (80) into Eq. (74)

$$\dot{\sigma} \cdot \varepsilon_0 + \dot{T}\Delta h + 2A\dot{z} = 2\lambda\dot{z} \tag{89}$$

In the case where no external stress is applied, at $T = M_s$, $z = 0$; and at $T = M_f$, $z = 1$. From Eq. (89), $\lambda = A + \Delta h(M_f - M_s)/2$. Similarly, at $T = A_s$, $z = 1$; and at $T = A_f$, $z = 0$. From Eq. (89), $\lambda = A - \Delta h(A_f - A_s)/2$. For simplicity, we may take the average value of λ as

$$\lambda = A + \frac{[(A_f + M_s) - (A_s + M_f)]}{4(T_2 - T_1)}(\sigma_2 - \sigma_1)\varepsilon_0 \tag{90}$$

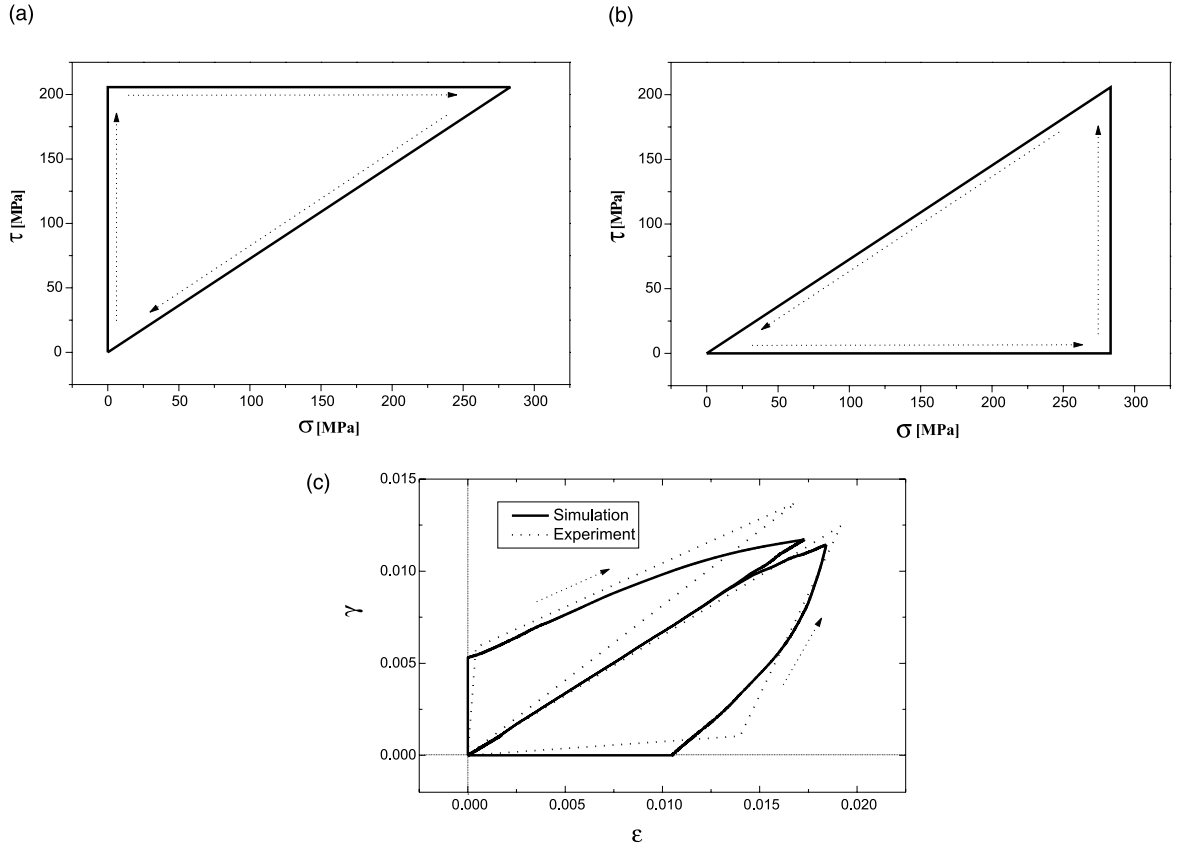

Fig. 11. (a) Imposed stress path, (b) imposed stress path and (c) strain path.

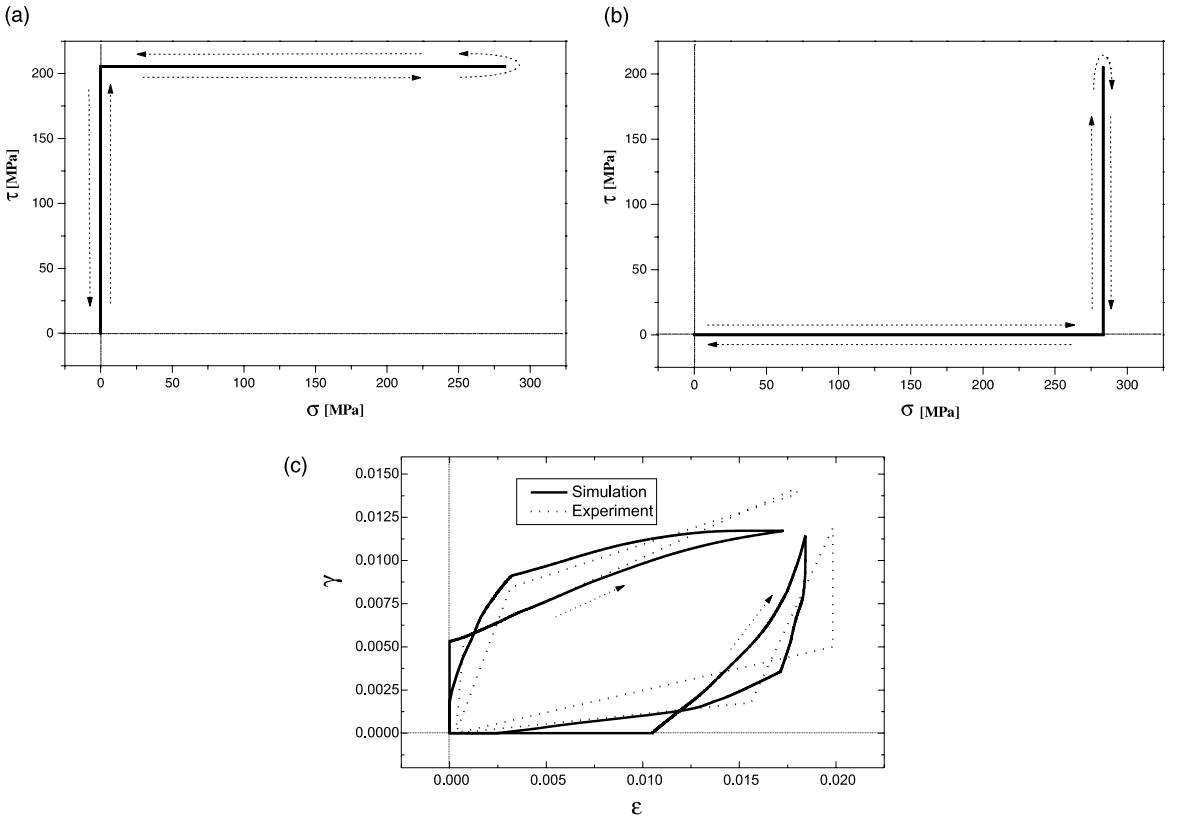

Fig. 12. (a) Imposed stress path, (b) imposed stress path and (c) strain path.

According to the experimental results in Sittner et al. (1995), we take $T = M_s$, $\sigma_1 = 0$, and $T_2 = T = 285$ K, $\sigma_2 = 239$ MPa.

The numerical results are compared with experiments in Figs. 4–13. As we can see, the simulation results are consistent with the measured results reported in Sittner et al. (1995). The numerical simulation shows that the proposed constitutive model is reliable in prediction the thermodynamic behavior of SMA under various complex loading conditions. The reason why there are some difference between simulation and experiment can be explained by the possible non-recoverable deformation (such as crystal slip, etc.) in the material.

Proposed model can also simulate shape memory effect. However, due to the lack of good experiment result, no simulation and comparison are presented here.

5. Conclusion

In this paper, a thermodynamic constitutive model for single crystalline and polycrystalline SMAs under complex thermomechanical load is presented. In this model, the material is studied at two different levels. If a SMA is austenite, it consists only austenite grains, which can be divided into different groups according to

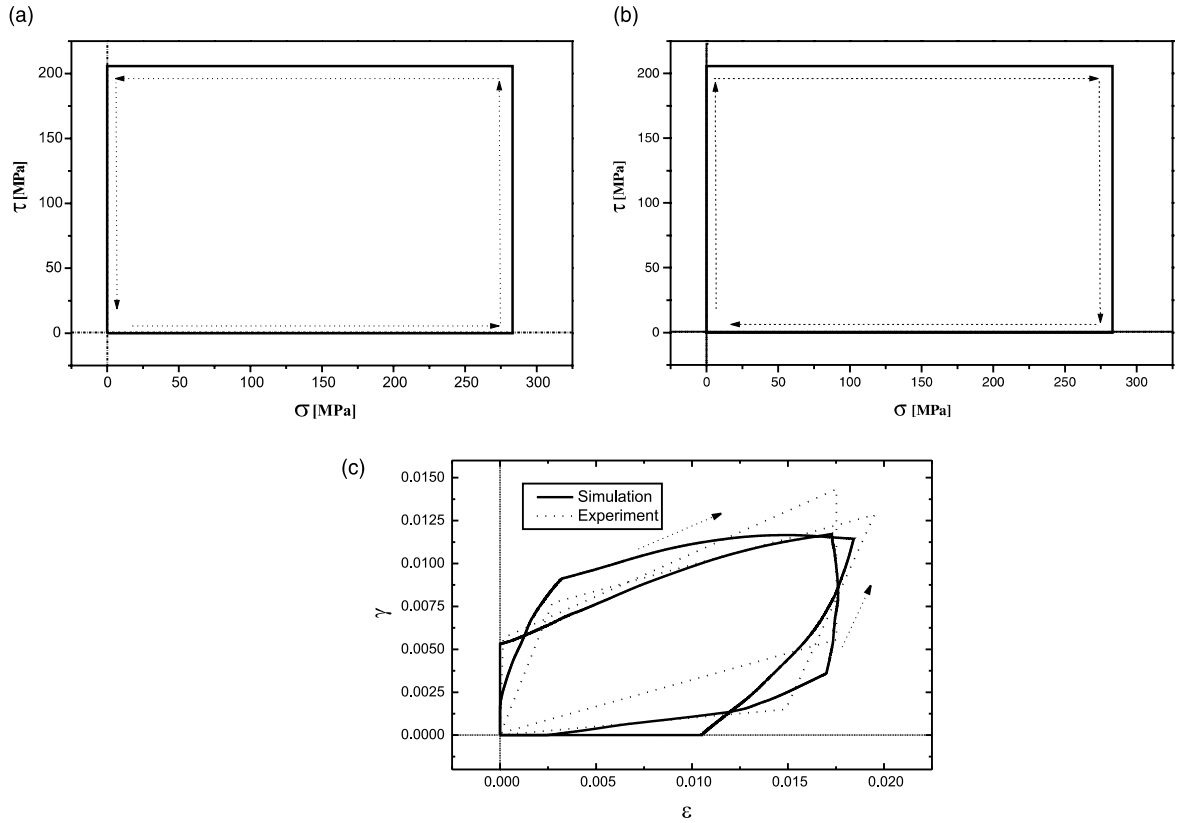

Fig. 13. (a) Imposed stress path, (b) imposed stress path and (c) strain path.

their grain orientations. When undergoing phase transformation, each group can be further divided into different subgroups according to different martensite variant induced. The volume fraction of each subgroup is chosen as internal variable to describe the evolution of phase transformation in the material. Volume average and variant combination methods are used in deriving the constitutive model. The transformation mechanism in each variant is considered the same as single variant phase transformation, no matter how complex the external loading condition is. This model can describe the thermomechanical behavior of SMAs under both proportional/non-proportional load, and cyclic load. Subsequently, a simplified version, i.e. orientation component model, is proposed for polycrystalline SMAs. This simplified model is used to simulate the response of a Cu–Al–Zn–Mn polycrystalline SMA round tube under proportional and non-proportional loads. Only one set of material parameters is used in all simulations. The results are consistent with experiments, which proves that the proposed model is reliable and convenient.

References

Abeyaratne, R., Knowles, J.K., 1993. A continuum model of a thermoelastic solid capable of undergoing phase transformation. J. Mech. Phys. Solids 44 (3), 541–571.

Ball, J.M., James, R.D., 1987. Fine phase mixtures as minimizers of energy. Arch. Rat. Mech. Anal. 100, 13–52.

Bhattacharya, K., 1992. Self-accommodation in martensite. Arch. Rat. Mech. Anal. 120, 201–244.

Boyd, J.G., Lagoudas, D.C., 1996. A thermodynamical constitutive model for shape memory materials. Int. J. Plast. 12 (6), 805–842.

Coleman, B.D., Gutin, M.E., 1967. Thermodynamics with internal state variables. J. Chem. Phys. 47, 597–613.
Funakubo, H., 1987. Shape memory alloys. Gordon and Breach Science Publishers, New York.
Gall, K., Sehitoglu, H., 1999. The role of texture in tension-compression asymmetry in polycrystalline NiTi. Int. J. Plast. 15 (10), 69–92.
Goo, B.C., Lexcellent, C., 1997. Micromechanics-based modeling of two-way memory effect of a single crystalline shape-memory alloy. Acta Mater. 45 (2), 727–737.
Huang, M., Brinson, L.C., 1998. A multivariant model for single crystal shape memory alloy behavior. J. Mech. Phys. Solids 46 (8), 1379–1409.
Huo, Y., Müller, I., 1993. Nonequilibrium thermodynamics of pseudoelasticity. Count. Mech. Thermodyn. 5 (1), 163–204.
Leclercq, S., Lexcellent, C., 1996. A general macroscopic description of the thermodynamical behavior of shape memory alloys. J. Mech. Phys. Solids 44 (6), 953–980.
Lexcellent, C., Goo, B.C., Sun, Q.P, Bernardini, J., 1996. Charcterization, thermodynamical behaviour and micromechanical-based constitutive model of shape-memory Cu–Zn–Al single crystals. Acta Mater. 44 (9), 3773–3780.
Liang, N.G., Song, H.T., Li, J., Liu. Z.H., 1995. Mesomechanical model for the constitutive behavior of polycrystalline shape memory alloys. In: Taminura, S., Khan, A.S. (Eds.), Dynamic Plasticity and Structural Behaviors, Amsterdam, pp. 625–628.
Liang, N.G., Liu, H.Q., Wang, T.C., 1998. A Meso elasto-plastic constitutive model for polycrystalline metals based on equivalent slip system with latent hardening. Sci. China, Ser. A 41A (8), 887–896.
Patoor, E., Eberhardt, A., Berveiller, M., 1995. Determination of the origin for the dissymmetry observed between tensile and compression tests on shape memory alloys. J. de Phys. C2 (5), 495–500.
Patoor, E., Eberhardt, A., Berveiller, M., 1998. Thermomechanical modelling of shape memory alloys. Arch. Mech. 40 (5–6), 7775–7794.
Raniecke, B., Lexcellent, C., 1994. RL-models of pseudoelasticity and their specification for some shape memory solids. Eur. J. Mech. A 13 (1), 21–50.
Rogers, R.C., 1996. Some remarks on nonlocal interactions and hysteresis in phase transitions. Count. Mech. Thermodyn. 8, 65–73.
Saburi, T., Nenno, S., 1982. The shape memory effect and related phenomena. In: Aaronson, H.I., et al., Proceedings International Conference on Solid to Solid Phase Transformation, pp. 1455–1479.
Seelecke, S., 1996. Equilibrium thermodynamics of pseudoelasticity and quasiplasticity. Count. Mech. Thermodyn. 8, 309–332.
Sittner, P., Hara, Y., Tokuda, M., 1995. Experimental study on the thermoelastic martensitic transformation in shape memory alloy polycrystal induced by combined external forces. Metall. Mat. Trans. 26, 2923–2935.
Sun, Q.P., Hwang, K.C., 1993. Micromechanics modelling for the constitutive behavior of polycrystalline shape memory alloys. J. Mech. Phys. Solids 41 (1), 1–33.
Tanaka, K., Nishmura, F., Tobushi, H., 1994. Phenomenological analysis and subloops in shape memory alloys due to incomplete transformations. J. Intell. Mater. Syst. Struct. 5, 487–493.